

# Baryon states with open charm in the extended local hidden gauge approach

W. H. Liang,<sup>1,\*</sup> T. Uchino,<sup>2</sup> C. W. Xiao,<sup>2</sup> and E. Oset<sup>2</sup>

<sup>1</sup>*Department of Physics, Guangxi Normal University,  
Guilin, 541004, People's Republic of China*

<sup>2</sup>*Departamento de Física Teórica and IFIC, Centro Mixto Universidad  
de Valencia-CSIC, Institutos de Investigación de Paterna,  
Apartado 22085, 46071 Valencia, Spain*

(Dated: June 7, 2019)

## Abstract

In this paper we examine the interaction of  $DN$ ,  $D\Delta$ ,  $D^*N$  and  $D^*\Delta$  states, together with their coupled channels, using an extension of the local hidden gauge formalism from the light meson sector, which is based on heavy quark spin symmetry. The scheme is based on the use of the impulse approximation at the quark level, with the heavy quarks acting as spectators, which occurs for the dominant terms where there is the exchange of a light meson. The pion exchange and the Weinberg Tomozawa interactions are generalized and with this dynamics we look for states generated from the interaction, finding two states with nearly zero width which are associated to the  $\Lambda_c(2595)$  and  $\Lambda_c(2625)$ . The lower state couples mostly to  $DN$ , and the second to  $D^*N$ . In addition to these two  $\Lambda_c$  states, we find four more states with  $I = 0$ , one of them nearly degenerate in two states of  $J = 1/2, 3/2$ . Furthermore we find seven states in  $I = 1$ , two of them degenerate in  $J = 1/2, 3/2$ , and other two degenerate in  $J = 1/2, 3/2, 5/2$ .

arXiv:1402.5293v1 [hep-ph] 21 Feb 2014

---

\* liangwh@gxnu.edu.cn

## I. INTRODUCTION

In dealing with hadronic states involving heavy quarks (charm or beauty) the heavy quark spin symmetry [1–4] plays an important role and serves as a guiding principle to proceed with calculations. Heavy quark spin symmetry (HQSS) has been applied to calculate baryon spectra in Refs. [5–12]. The basic idea behind these works is to use HQSS to reduce the freedom in the interaction, which is then written in terms of a few parameters which are adjusted to some experimental data. Then predictions on spectra of baryons with charm or beauty, or hidden charm and beauty are made. In Ref. [5] an SU(8) spin-flavor scheme is used, to account for the spin symmetry, in order to obtain the interaction, and a coupled channel unitary approach is implemented to obtain poles in the scattering matrices, which correspond to the baryon resonance states. In particular the  $\Lambda_c(2595)$  state is obtained and shown to couple largely to the  $D^*N$  channel. In Ref. [8] the SU(8) scheme is once again used, but with some symmetry breaking, to match with an extension of the Weinberg Tomozawa interaction in SU(3). Among other resonances, the states  $\Lambda_c(2595)$  ( $J^P = 1/2^-$ ) and  $\Lambda_c(2625)$  ( $J^P = 3/2^-$ ) are obtained.

Further steps on the relationship of the Weinberg Tomozawa interaction and HQSS are given in Refs. [10, 13], where it is shown that this interaction, which stems from the exchange of vector mesons in the local hidden gauge approach [14–16] (see also Ref. [17] for practical rules), fulfills the HQSS. Indeed, the dominant terms correspond to the exchange of light vectors (the exchange of heavy vectors is suppressed), the heavy quarks act as spectators and hence the interaction does not depend upon them. HQSS is then automatically fulfilled. Another step forward in this direction was given in Ref. [18], where using the impulse approximation at the quark level, the Weinberg Tomozawa interaction of the SU(3) sector was extended to the heavy bottom sector and it was shown that the result is equivalent to the plain use of the local hidden gauge approach extended to SU(4)<sup>1</sup>. It was also shown in Ref. [18] that the case of pion exchange requires a renormalization due to the field normalization of the mesons, which is automatically implemented in the Weinberg Tomozawa term. Another novelty in Ref. [18] was to realize that a better measure of the relevance of different channels in the wave function of the states is to look at the wave function at the origin, rather than the coupling from the residues at the pole of the different amplitudes. These findings are most welcome and a posteriori justify the approaches used in many works where the Weinberg Tomozawa interaction has been used in the heavy quark sector [19–25], or variants of it, as in the Jülich model [26, 27].

In Ref. [18] the states  $\Lambda_b(5912)$  and  $\Lambda_b(5920)$  were obtained, among others, using a unitary scheme with coupled channels and the dynamics based on the local hidden gauge approach. These states in ( $J^P = 1/2^-, 3/2^-$ ) respectively were naturally obtained in the  $\bar{B}^*N$  and coupled channels sector, and the difference of masses comes from the different weight of the intermediate  $\bar{B}N$  states, which are accounted for by means of box diagrams mediated by pion exchange.

In the charm sector we have states which bear some similarity with those states in the beauty sector. They are the  $\Lambda_c(2595)$  ( $J^P = 1/2^-$ ) and  $\Lambda_c(2625)$  ( $J^P = 3/2^-$ ) states which have been observed in various experiments [28]. It is tempting to see if a similar explanation can be given in this case, or see if those states call for a different explanation. We anticipate that although there are similarities, there are also differences and, while the  $\Lambda_c(2625)$  ( $J^P = 3/2^-$ ) state is mostly tied to the  $D^*N$  channel, the  $\Lambda_c(2595)$  state has a

<sup>1</sup> Actually one only needs to use SU(3) once the heavy quarks act as spectators.

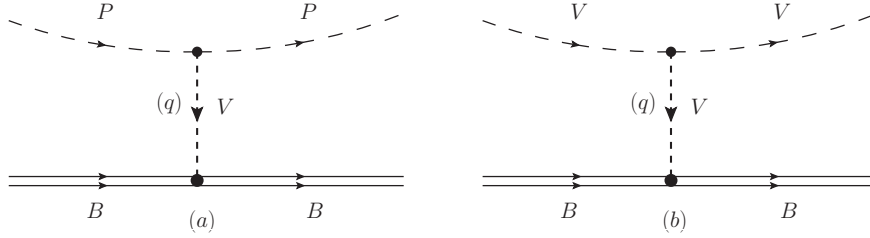


FIG. 1. Diagrammatic representation of the pseudoscalar baryon interaction (a) and vector baryon interaction (b).

more important coupling to the  $DN$  channel. The existence of these two states allows us to constrain the only free parameters of our model and after this we make predictions for other states in isospin  $I = 0$  and  $I = 1$ .

## II. FORMALISM

We take as basis of states  $\pi\Sigma_c, \pi\Lambda_c, \eta\Lambda_c, \eta\Sigma_c, DN$  which can couple to  $I = 0, 1$ . Similarly, we consider  $D^*N$  and  $\pi\Sigma_c^*, \eta\Sigma_c^*, D\Delta, D^*\Delta$ , with  $\Delta \equiv \Delta(1232)$  and  $\Sigma_c^* = \Sigma_c^*(2520)$ , belonging to a decuplet of  $3/2^+$  states. In the local hidden gauge approach in  $SU(3)$  [14–16] the meson baryon interaction proceeds via the exchange of vector mesons as depicted in Fig. 1. As discussed in Ref. [18], when we exchange a light vector meson in diagram (a), (b) of Fig. 1, the heavy quarks of the meson or the baryon are spectators and, as a consequence, the interaction does not depend on their spin-flavor. Technically, the interaction of the diagrams of Fig. 1 can be obtained using  $SU(3)$  symmetry considering  $u, d, c$  quarks, since we do not consider states with strangeness or hidden strangeness. Hence, all the matrix elements of the interaction are identical (except for the mass or energy dependence) to those of the interaction of the analogous states  $\pi\Sigma, \pi\Lambda, \eta\Lambda, \eta\Sigma, \bar{K}N, \bar{K}^*N, \pi\Sigma^*, \eta\Sigma^*, \bar{K}\Delta, \bar{K}^*\Delta$ , which have been studied in Refs. [29, 30].

The transition potential from channel  $i$  to channel  $j$  is given by [31]

$$V = -C_{ij} \frac{1}{4f^2} (2\sqrt{s} - M_{B_i} - M_{B_j}) \sqrt{\frac{M_{B_i} + E_i}{2M_{B_i}}} \sqrt{\frac{M_{B_j} + E_j}{2M_{B_j}}}, \quad (1)$$

with  $f$  the pion decay constant,  $M_{B_i}, E_i$  ( $M_{B_j}, E_j$ ) the mass, energy of baryon of  $i$  ( $j$ ) channel. We take  $f = f_\pi = 93$  MeV since we exchange light vector mesons. The  $C_{ij}$  coefficients are evaluated in Refs. [29, 30] and we quote them below. We note that, according to [18], one must use  $f_\pi$ , since the corrections due the consideration of heavy hadrons are automatically taken into account in the energy dependence of the interaction (note that Eq. (1) provides a relativistic version of the sum of the two external meson energies).

For pseudoscalar mesons and  $1/2^+$  baryons we have the coupled channels  $DN, \pi\Sigma_c, \eta\Lambda_c$  in  $I = 0$  and the  $C_{ij}$  coefficients are given in Table I.

$C_{ij}$	$DN$	$\pi\Sigma_c$	$\eta\Lambda_c$
$DN$	3	$-\sqrt{\frac{3}{2}}$	$\frac{3}{\sqrt{2}}$
$\pi\Sigma_c$		4	0
$\eta\Lambda_c$			0

TABLE I.  $C_{ij}$  coefficients for  $I = 0$  and  $J^P = 1/2^-$ .

In  $I = 1$  we have the channels  $DN$ ,  $\pi\Sigma_c$ ,  $\pi\Lambda_c$ ,  $\eta\Sigma_c$  and the  $C_{ij}$  coefficients are given in Table II.

$C_{ij}$	$DN$	$\pi\Sigma_c$	$\pi\Lambda_c$	$\eta\Sigma_c$
$DN$	1	-1	$-\sqrt{\frac{3}{2}}$	$-\sqrt{\frac{3}{2}}$
$\pi\Sigma_c$		2	0	0
$\pi\Lambda_c$			0	0
$\eta\Sigma_c$				0

TABLE II.  $C_{ij}$  coefficients for  $I = 1$  and  $J^P = 1/2^-$ .

We can see that the interaction in  $I = 0$  is stronger than in  $I = 1$  and one has more chances to bind states in  $I = 0$ .

As discussed in Ref. [10], the mixing of baryons of the octet (in  $u$ ,  $d$ ,  $c$ ) like  $\Sigma_c$  and of the decuplet  $\Sigma_c^*$  requires pion exchange, which is suppressed in the heavy quarks sector. However, it was shown in Ref. [18] that this mixing was responsible for the breaking of the original degeneracy of two spin states of  $\Lambda_b$ , which upon consideration of this mixing became the  $\Lambda_b(5912)$  and  $\Lambda_b(5920)$ . We will discuss this mixing in Section IV.

When we consider a pseudoscalar meson and a baryon of the decuplet, we have the results for  $C_{ij}$  given in Tables III and IV [30]. We note that the strength of the  $D\Delta \rightarrow D\Delta$  coefficient is four times bigger than for  $DN \rightarrow DN$  and hence, we should expect larger bindings in this case.

$C_{ij}$	$\pi\Sigma_c^*$
$\pi\Sigma_c^*$	4

TABLE III.  $C_{ij}$  coefficient for  $I = 0$  and  $J^P = 3/2^-$ .

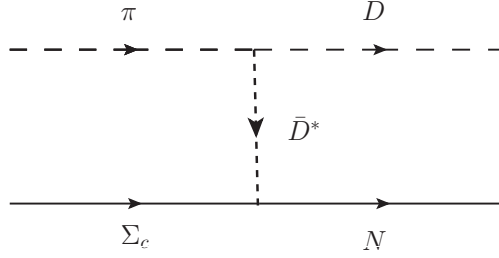


FIG. 2. Transition potential from  $\pi\Sigma_c \rightarrow DN$ .

$C_{ij}$	$D\Delta$	$\pi\Sigma_c^*$	$\eta\Sigma_c^*$
$D\Delta$	4	1	$\sqrt{6}$
$\pi\Sigma_c^*$		2	0
$\eta\Sigma_c^*$			0

TABLE IV.  $C_{ij}$  coefficients for  $I = 1$  and  $J^P = 3/2^-$ .

We do not consider the interaction  $D\Delta$  and coupled channels with  $I = 2$  which is found repulsive in our approach.

In coupled channels we make use of the Bethe-Salpeter equation

$$T = [1 - VG]^{-1}V, \quad (2)$$

with  $G$  the diagonal loop function for the propagating intermediate meson baryon channels. In Ref. [13] a warning was raised about potential dangers of using the dimensional regularization for the  $G$  functions (see also Ref. [25]). This was so because for values of the energy below threshold,  $G$  can become positive and then one can obtain bound states with a positive (repulsive) potential when  $1 - VG = 0$ , which is not physically acceptable (see Eq. (2) in one channel). Hence, we use here the cut off regularization for  $G$  given by

$$G(s) = \int_0^{q_{max}} \frac{d^3\vec{q}}{(2\pi)^3} \frac{\omega_P + \omega_B}{2\omega_P\omega_B} \frac{2M_B}{P^0 - (\omega_P + \omega_B)^2 + i\epsilon}, \quad (3)$$

where  $\omega_P = \sqrt{\vec{q}^2 + m_P^2}$ ,  $\omega_B = \sqrt{\vec{q}^2 + M_B^2}$ , and  $q_{max}$  is the cut-off of the three-momentum.

Before closing this sector we must mention some feature concerning the transition  $\pi\Sigma_c \rightarrow DN$ . This is depicted in Fig. 2. and it is mediated by  $\bar{D}^*$  exchange in the extended local hidden gauge approach. If we followed the strict large heavy quark mass counting we would neglect this term because it involves the exchange of a heavy vector  $\bar{D}^*$  and its propagator would make this term small. However, although the term is suppressed, it is not as much as one would expect. Indeed, the propagator will be

$$D_{D^*} = \frac{1}{p_{D^*}^2 - m_{D^*}^2} \equiv \frac{1}{(p_\pi^0 - p_D^0)^2 - (\vec{p}_\pi - \vec{p}_D)^2 - m_{D^*}^2}. \quad (4)$$

Conversely, in a diagonal transition  $DN \rightarrow DN$  mediated by  $\rho$  exchange, for instance, we have

$$D_\rho \approx \frac{1}{m_V^2}. \quad (5)$$

Thus, close to  $DN$  threshold the ratio is

$$\frac{D_{D^*}}{D_\rho} \simeq \frac{m_V^2}{(p_\pi^0 - p_D^0)^2 - \vec{p}_\pi^2 - m_{D^*}^2} \simeq \frac{1}{4}. \quad (6)$$

This ratio was already noticed in Ref. [21]. Since the non diagonal terms have a smaller importance in the process than the diagonal ones of the heavy mesons, we simply account for these transitions multiplying by 1/4 the results obtained from Eq. (1) and the Tables.

### III. VECTOR-BARYON CHANNELS

The transitions  $VB \rightarrow VB$  for small three-momenta of the external vector mesons have formally the same expressions as the corresponding  $PB \rightarrow PB$  substituting the octet of pseudoscalars by the octet of vectors [32]. There is only one minor change needed to account for the  $\phi$  and  $\omega$  SU(3) structure, which is to replace each  $\eta$  by  $-\sqrt{2/3} \phi$  or  $\sqrt{1/3} \omega$ . The case of vector interaction with the decuplet of baryons is similar [33]. In this case, the Tables I, II, IV are changed to Tables V, VI, VII. Once again we suppress with a factor 1/4 the transitions from a heavy vector to a light vector as done before for the pseudoscalar mesons.

$C_{ij}$	$D^*N$	$\rho\Sigma_c$	$\omega\Lambda_c$	$\phi\Lambda_c$
$D^*N$	3	$-\sqrt{\frac{3}{2}}$	$\sqrt{\frac{3}{2}}$	$-\sqrt{3}$
$\rho\Sigma_c$		4	0	0
$\omega\Lambda_c$			0	0
$\phi\Lambda_c$				0

TABLE V.  $C_{ij}$  coefficients for  $D^*N$  and coupled channels for  $I = 0$ , and  $J^P = 1/2^-, 3/2^-$ .

$C_{ij}$	$D^*N$	$\rho\Sigma_c$	$\rho\Lambda_c$	$\omega\Sigma_c$	$\phi\Sigma_c$
$D^*N$	1	-1	$-\sqrt{\frac{3}{2}}$	$-\sqrt{\frac{1}{2}}$	1
$\rho\Sigma_c$		2	0	0	0
$\rho\Lambda_c$			0	0	0
$\omega\Sigma_c$				0	0
$\phi\Sigma_c$					0

TABLE VI.  $C_{ij}$  coefficients for  $D^*N$  and coupled channels for  $I = 1$ , and  $J^P = 1/2^-, 3/2^-$ .

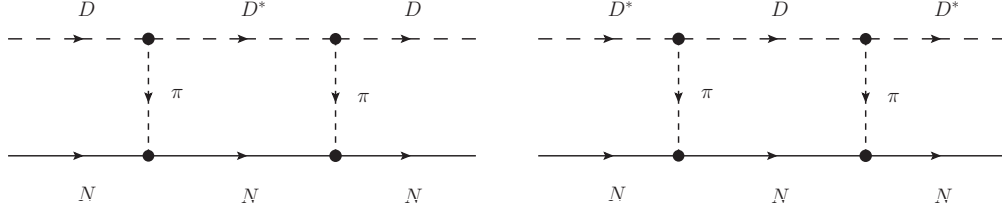


FIG. 3. Diagrammatic representation of the  $D^*N$  in intermediate state (left) and the  $DN$  in intermediate state (right).

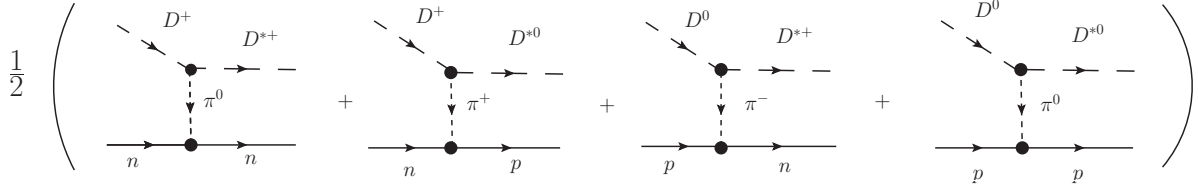


FIG. 4. Diagrammatic representation of the transition  $DN \rightarrow D^*N$  in  $I = 0$ .

$C_{ij}$	$D^*\Delta$	$\rho\Sigma_c^*$	$\omega\Sigma_c^*$	$\phi\Sigma_c^*$
$D^*\Delta$	4	1	$\sqrt{2}$	-2
$\rho\Sigma_c^*$		2	0	0
$\omega\Sigma_c^*$			0	0
$\phi\Sigma_c^*$				0

TABLE VII.  $C_{ij}$  coefficients for  $D^*\Delta$  and coupled channels for  $I = 1$ , and  $J^P = 1/2^-, 3/2^-, 5/2^-$ .

#### IV. BREAKING THE $J = 1/2^-, 3/2^-$ DEGENERACY IN THE $D^*N$ SECTOR

In this section we break the degeneracy of the  $1/2^-, 3/2^-$  states of the  $D^*N$  sector. We follow the approach of Ref. [34–37] and mix states of  $D^*N$  and  $DN$  in both spin channels. We, thus, evaluate the contribution of the box diagrams of Fig. 3, in analogy to the box diagrams evaluated in Ref. [34], and add this contribution,  $\delta V$ , to the  $DN$  or  $D^*N$  potential. Using the doublets of isospin  $(\bar{D}^0, D^-)$ ,  $(D^+, -D^0)$  the  $\Lambda_c$  state in the  $DN$  basis is given by

$$|DN, I = 0\rangle = \frac{1}{\sqrt{2}}(|D^+n\rangle + |D^0p\rangle), \quad (7)$$

and analogously for  $D^*N$ . The  $DN \rightarrow D^*N$  transition in  $I = 0$  is given by the diagrams of Fig. 4.

The  $VP\pi$  vertex in  $SU(3)$  is given by the Lagrangian

$$\mathcal{L}_{VPP} = -ig \langle [P, \partial_\mu P] V^\mu \rangle, \quad (8)$$

where  $P$ ,  $V^\mu$  are the ordinary meson octet and vector nonet  $SU(3)$  matrix of the correspond-

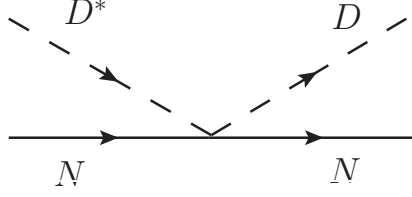


FIG. 5. Diagram of the Kroll Ruderman term.

ing fields

$$P = \begin{pmatrix} \frac{\pi^0}{\sqrt{2}} + \frac{\eta_8}{\sqrt{6}} & \pi^+ & K^+ \\ \pi^- & -\frac{\pi^0}{\sqrt{2}} + \frac{\eta_8}{\sqrt{6}} & K^0 \\ K^- & \bar{K}^0 & -\frac{2\eta_8}{\sqrt{6}} \end{pmatrix}, \quad (9)$$

$$V_\mu = \begin{pmatrix} \frac{\rho^0}{\sqrt{2}} + \frac{\omega}{\sqrt{2}} & \rho^+ & K^{*+} \\ \rho^- & -\frac{\rho^0}{\sqrt{2}} + \frac{\omega}{\sqrt{2}} & K^{*0} \\ K^{*-} & \bar{K}^{*0} & \phi \end{pmatrix}_\mu. \quad (10)$$

and  $g = m_V/2f_\pi$  with  $m_V \approx 780$  MeV,  $f_\pi = 93$  MeV. One can extend the Lagrangian Eq. (8) to the SU(4) space, as done in Ref. [38], but it is unnecessary. In Ref. [18] it was shown how to extend to the heavy sector the results of SU(3), using the impulse approximation at the quark level and considering the heavy quarks as spectators. The result obtained was that the  $K^{*+} \rightarrow K^0\pi^+$  and  $B^{*+} \rightarrow B^0\pi^+$  transition amplitudes were related by the relationship

$$\frac{t_{B^*}}{t_{K^*}} \equiv \frac{\sqrt{m_{B^*}m_B}}{\sqrt{m_{K^*}m_K}} \simeq \frac{m_{B^*}}{m_{K^*}}. \quad (11)$$

In our case this ratio is changed to  $m_{D^*}/m_{K^*}$ . It was also found in Ref. [18] that the ratio of energies that must be implemented in the ratio of amplitudes for the Weinberg Tomozawa term was already provided by the form of the Weinberg Tomozawa amplitude, Eq. (1), that incorporates the energy of the mesons explicitly as a factor.

Now we come back to the evaluation of the box diagrams of Fig. 3. The vertex for the  $I = 0$  transition  $DN \rightarrow D^*N$  of Fig. 4, considering the Yukawa coupling for the  $\pi NN$  vertex is given by

$$-it = -\frac{3}{\sqrt{2}}g \frac{m_{D^*}}{m_{K^*}}(q + P_{in})_\mu \epsilon^\mu \frac{1}{q^2 - m_\pi^2} \frac{D + F}{2f_\pi} \vec{\sigma} \cdot \vec{q}, \quad (12)$$

with  $D = 0.75$  and  $F = 0.51$  [39], and since  $P_{in} = q + P_{out}$  and  $P_{out} \cdot \epsilon = 0$  plus  $\epsilon^0 \approx 0$ , we get effectively

$$-it = \frac{6}{\sqrt{2}}g \frac{m_{D^*}}{m_{K^*}} \vec{q} \cdot \vec{\epsilon} \frac{1}{q^2 - m_\pi^2} \frac{D + F}{2f_\pi} \vec{\sigma} \cdot \vec{q}. \quad (13)$$

In addition to the pion exchange of Fig. 4, we have the Kroll Ruderman contact term, depicted in Fig. 5. Following Refs. [34, 40], in order to get the Kroll Ruderman term we must substitute in Eq. (12)  $\epsilon_\mu(q + P_{in})^\mu \frac{1}{q^2 - m_\pi^2} \vec{\sigma} \cdot \vec{q}$  by  $-\vec{\sigma} \cdot \vec{q}$ . Then, we must evaluate the diagrams of Fig. 6 and we obtain



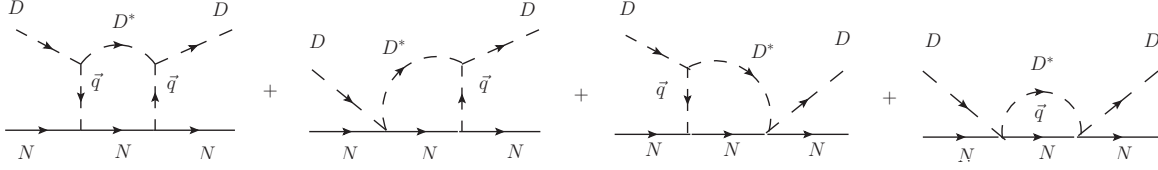


FIG. 6. All the diagrams for  $D^*N$  in the intermediate state.

$$\delta V = \delta V^{PP} + 2\delta V^{PC} + \delta V^{CC}, \quad (14)$$

where  $\delta V^{PP}$  stands for the first diagram of Fig. 6,  $2\delta V^{PC}$  for the two middle diagrams and  $\delta V^{CC}$  for the last one. The expressions for these terms can be seen in section V of Ref. [18]. All that is needed is to change the masses of  $\bar{B}$  and  $\bar{B}^*$  by those of  $D$  and  $D^*$ .

## V. BOX DIAGRAM FOR $I = 1$ STATES

We now evaluate the contribution of the box diagram to the  $I = 1$  states made from  $DN$ ,  $D^*N$ ,  $D\Delta$ ,  $D^*\Delta$ .

a)  $DN$ ,  $I = 1$ :

The isospin  $I = 1$  state is now

$$|DN; I = 1, I_3 = 0\rangle = \frac{1}{\sqrt{2}}(|D^+n\rangle - |D^0p\rangle). \quad (15)$$

The counting of isospin done before for the  $D^* \rightarrow D\pi$  transition can be repeated and we simply find that a factor  $\frac{3}{\sqrt{2}}$  gets converted in  $\frac{1}{\sqrt{2}}$  in the  $DN \rightarrow D^*N$  transition. We thus get a factor 9 smaller contribution than for  $I = 0$  from the box and we neglect it.

b)  $D^*N$ ,  $I = 1$ :

We have the same suppression factor as before and we also neglect it.

c)  $D\Delta$ ,  $I = 1$ :

The state of  $D\Delta$  with  $I = 1$  is given by

$$|D\Delta; I = 1, I_3 = 1\rangle = \sqrt{\frac{3}{4}}|D^0\Delta^{++}\rangle + \sqrt{\frac{1}{4}}|D^+\Delta^+\rangle. \quad (16)$$

The diagram under contribution is now in Fig. 7. We must also substitute  $\frac{f}{m_\pi}\vec{\sigma} \cdot \vec{q}\tau^\lambda$  in the case of nucleons by  $\frac{f_\Delta}{m_\pi}\vec{S}_\Delta \cdot \vec{q}T_\Delta^\lambda$ , where  $\vec{S}_\Delta$ ,  $\vec{T}_\Delta$  are the ordinary spin and isospin matrices of the  $\Delta$ .

We have [41]

$$\frac{f_\Delta}{f} = \frac{4}{5}, \quad (\text{where } \frac{f}{m_\pi} = \frac{F + D}{2f}). \quad (17)$$

Once again, the expression that we get for this contribution can be seen in section VII of Ref. [18], simply changing the mass of the  $\bar{B}^*$  to that of  $D^*$ .

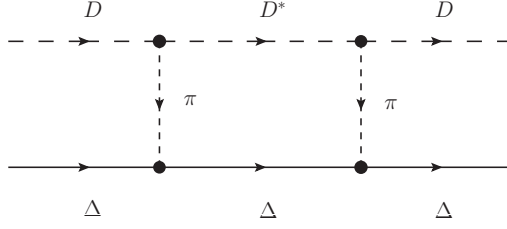


FIG. 7. Diagrammatic representation of the transition of  $D\Delta \rightarrow D^*\Delta \rightarrow D\Delta$ .

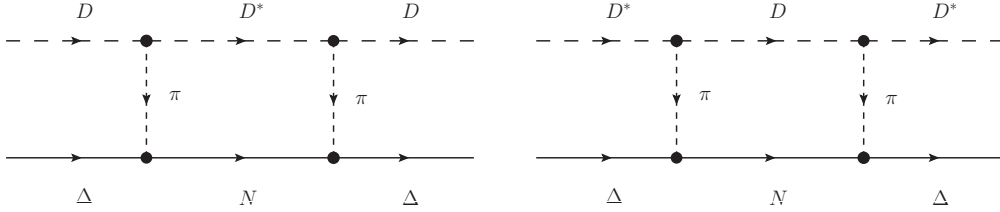


FIG. 8. Diagrammatic representation of the  $D^*N$  in intermediate state (left) and the  $DN$  in intermediate state (right).

## VI. FURTHER DECAY CHANNELS OF $D\Delta$ AND $D^*\Delta$

In this section we evaluate the box diagram corresponding to Figs. 8. We thus consider the intermediate  $DN$  or  $D^*N$  channels. Should the binding  $D\Delta$  and  $D^*\Delta$  states be not bigger than the  $\Delta$  and  $N$  mass difference,  $DN$  and  $D^*N$  would provide decay channels of the states. In principle we should also consider the  $D\Delta$  and  $D^*\Delta$  intermediate states for the  $DN$  and  $D^*N$  states, but, considering the binding, these intermediate states are about 600 MeV away in energy and we do not consider them. The changes to be done are also simple: we must substitute

$$\frac{f}{m_\pi} \vec{\sigma} \cdot \vec{q} \tau^\lambda \rightarrow \frac{f_{\pi N \Delta}}{m_\pi} \vec{S} \cdot \vec{q} T^\lambda, \quad (18)$$

where now  $\vec{S} (\vec{T})$  is transition spin (isospin) operator from spin (isospin)  $3/2$  to  $1/2$ , with the normalization for  $S_\mu^+$  in spherical basis

$$\langle 3/2 M | S_\mu^+ | 1/2 m \rangle = \mathcal{C}(1/2 \ 1 \ 3/2; m_\mu \ M), \quad (19)$$

with  $\mathcal{C}(\cdot)$  a Clebsch-Gordan coefficient, and we have the property [42]

$$\sum_M S_i |M\rangle \langle M| S_j = \frac{2}{3} \delta_{ij} - i \frac{1}{3} \epsilon_{ijk} \sigma_k, \quad (20)$$

for  $S_i, S_j$  in cartesian basis. Also from Ref. [42] we take  $f_{\pi N \Delta}/f = 2.25$ . For the isospin transition, in addition to the  $I = 1$   $D\Delta$  state of Eq. (16) we need

$$|DN; I = 1, I_3 = 1\rangle = |D^+p\rangle. \quad (21)$$

Once again, the expressions for the terms obtained can be found in section VIII of Ref. [18] with trivial changes of the masses.

## VII. RESULTS FOR $I = 0$

In Table VIII we show the results that we obtain for  $J = 1/2, I = 0$  from the  $DN$  and coupled channels as a function of the cut off,  $q_{max}$ , used. In the Table we show the results obtained with and without the box. In the  $s$ -wave amplitude that we study, the parity of all the states obtained is negative.

$q_{max}$	600	630	638	700	750
no box	$2602.5 + i34.8$	$2599.7 + i27.8$	$2598.8 + i25.6$	$2590.8 + i0$	$2562.5 + i0$
	$2685.5 + i5.3$	$2666.8 + i7.7$	$2661.8 + i8.7$	$2629.4 + i21.5$	$2616.7 + i25.7$
with box	$2603.2 + i30.1$	$2597.6 + i11.0$	$2592.0 + i4.5$	$2547.2 + i0$	$2498.9 + i0$
	$2647.0 + i9.5$	$2625.2 + i22.8$	$2623.3 + i26.4$	$2612.0 + i31.0$	$2604.9 + i26.9$

TABLE VIII. Poles in coupled channels  $DN(2806)$ ,  $\pi\Sigma_c(2592)$ ,  $\eta\Lambda_c(2834)$  with  $I = 0$  as a function of  $q_{max}$ . (The number in brackets after the channel is the mass of the channel. Units: MeV)

We can see that for  $q_{max} = 638$  MeV, and considering the box, we obtain a state with small width of 9 MeV. This state could be associated with the experimental one  $\Lambda_c(2595)$ , which has a mass of  $2592.25 \pm 0.28$  MeV and a width of 2.59 MeV. The effect of the box has been a reduction of the mass by about 7 MeV, which indicates a small mixing with  $D^*N$ .

It is interesting to observe in this Table that we predict another  $J = 1/2, I = 0$  state with a mass of 2623 MeV and a width of 53 MeV.

One may complain that the width of the 2592 MeV state that we get is larger than the experimental one, but we are very close to the  $\pi\Sigma_c$  threshold and the results are very sensitive to the precise value of the mass of the state. For these reasons we make a small variation of  $q_{max}$  around 640 MeV and show the results in Table IX .

$q_{max}$	645	650	655	660	670
no box	$2597.8 + i23.5$	$2597.3 + i21.9$	$2596.6 + i20.1$	$2595.7 + i18.2$	$2593.7 + i14.0$
	$2657.4 + i9.6$	$2654.3 + i10.4$	$2651.2 + i11.2$	$2648.2 + i12.2$	$2642.4 + i14.4$
with box	$2591.2 + i0$	$2588.8 + i0$	$2585.5 + i0$	$2581.9 + i0$	$2573.9 + i0$
	$2621.9 + i28.4$	$2620.9 + i29.4$	$2620.0 + i30.2$	$2619.1 + i30.8$	$2617.2 + i31.4$

TABLE IX. Poles in coupled channels  $DN(2806)$ ,  $\pi\Sigma_c(2592)$ ,  $\eta\Lambda_c(2834)$  with  $I = 0$  as a function of  $q_{max}$ . (The number in brackets after the channel is the mass of the channel. Units: MeV)

We can see that taking  $q_{max} = 645$  MeV reduces the mass of the state by 0.8 MeV, and being below the  $\pi\Sigma_c$  threshold, the width is now zero. The channel  $\pi\Sigma_c$  is what gives width to the state and the proximity to the threshold is what makes the width very small.

In Table X we show now the results for the states of  $J = 1/2, 3/2, I = 0$ , obtained from the  $D^*N$  interaction with its coupled channels, both with inclusion or not of the box diagram. We obtain two states, degenerate in spin without the box. The box diagram breaks

the degeneracy for the lower energy state but barely changes the result for the higher energy state, something that we shall be able to interpret when we look at the couplings of the states to the different channels. The reason for the breakup of the spin degeneracy is the Kroll Ruderman term that only acts in  $J = 1/2$ . The effect of the box is a reduction of the mass of this lower energy state by about 60 MeV for values of  $q_{max}$  around 800 MeV. The effect of the box is bigger here than in the former case. First we are choosing  $q_{max}$  bigger, but also the mass of  $DN$  in the intermediate state is closer here to the energies obtained than the mass of  $D^*N$  to the energies of Table VIII. We are searching for the experimental  $J = 3/2$ ,  $\Lambda_c(2625)$ , which has a mass of  $2628.11 \pm 0.19$  MeV and a width smaller than 0.97 MeV. We find a candidate with zero width for  $q_{max} = 791$  MeV. In addition we obtain three more states, since we obtain two states with  $J = 1/2$  and two with  $3/2$ , all of them with zero or very small width. The effect of the box is very small in the higher energy state, which is then nearly degenerate in  $J = 1/2$  and  $3/2$ . We shall be able to interpret this when we look for the couplings of the states to the different channels.

$q_{max}$	750	780	791	810	850
no box	$2707.9 + i0$	$2683.1 + i0$	$2673.9 + i0$	$2657.9 + i0$	$2624.0 + i0$
	$2984.7 + i0.5$	$2966.4 + i0.4$	$2959.8 + i0.3$	$2948.6 + i0.1$	$2926.0 + i0$
with box ( $J = 1/2$ )	$2654.5 + i0$	$2626.0 + i0$	$2615.4 + i0$	$2596.9 + i0$	$2557.6 + i0$
	$2984.2 + i0.9$	$2965.8 + i0.8$	$2959.1 + i0.7$	$2947.9 + i0.6$	$2925.0 + i0.7$
with box ( $J = 3/2$ )	$2663.8 + i0$	$2638.0 + i0$	$2628.5 + i0$	$2611.9 + i0$	$2576.5 + i0$
	$2983.6 + i1.6$	$2965.2 + i1.5$	$2958.6 + i1.5$	$2947.4 + i1.4$	$2924.3 + i1.4$

TABLE X. Poles in coupled channels  $D^*N(2948)$ ,  $\rho\Sigma_c(3229)$ ,  $\omega\Lambda_c(3069)$ ,  $\phi\Lambda_c(3306)$  with  $I = 0$  as a function of  $q_{max}$ . (Units: MeV)

The first striking thing is that we have used two different cut offs in the two sectors. Although they are still rather similar, this might look a bit arbitrary, but the regularization scale does not have to be exactly the same for different sectors. What we have done is to use two free parameters of the theory to fine tune the energies of the two states, but we would not have claimed success if the cut off needed had been outside the natural range. Even then, it is by no means trivial to get the width so small, as in the experiment. Note that in the case of the  $DN$  states we also found a state with a mass of the order of 2623 MeV but the width was about 52 MeV. Yet, it is interesting to recall that the values of the cut off needed to get these states are perfectly in line with what was already observed in the light sector. Indeed, in the study of the  $\bar{K}N$  interaction with its coupled channels, two states for the  $\Lambda(1405)$  were obtained in Ref. [43] using the input of Ref. [29], the one at 1420 MeV corresponding to the  $\Lambda_c(2595)$  obtained here. The cut off needed in Ref. [29] was 630 MeV, much in line with what we have found here. On the other hand, an analogous case to the spin 1/2, 3/2 that we obtain from the  $D^*N$  and coupled channels is the one of the resonances  $\Delta(1900)(1/2^-)$ ,  $\Delta(1930)(5/2^-)$ ,  $\Delta(1940)(3/2^-)$ . These states were studied along the same lines as here in Ref. [44] with the  $\rho\Delta$  channel, and with extra coupled channels in Ref. [33],

and a cut off of about 770 MeV was needed to reproduce them. In other studies a different regularization procedure is done by making the  $G$  function zero at  $\sqrt{s} = \sqrt{m_M^2 + m_B^2}$ , where  $m_M, m_B$  are the meson and baryon masses for the lightest of the coupled channels in a given quantum number [5, 19]. In practice this has a similar effect to the one of the different cut offs.

It is interesting to see in Table X that we obtain a state at 2615 MeV with  $J = 1/2$  and zero width. This is not far away from the  $J = 1/2$  state of Table VIII at 2592 MeV, and one might think that this could be a candidate for the experimental 2595 MeV state, given the flexibility of the theory to make small changes in the cut off. However, there is one argument against this interpretation. This state is linked to the 2628 MeV,  $J = 3/2$  state of Table X. Once this latter energy is fixed, so is the one of the  $J = 1/2$  state. One might think that a compromise for the two spin states could be found with a different cut off, but this is not possible because the difference of mass of these two states in the range of  $q_{max} = 780 - 850$  MeV (not to spoil too much the agreement for the 3/2 state) ranges within 12-19 MeV, rather stable with the cut off, while the difference between the experimental 1/2 and 3/2 states is 36 MeV. This fact, however, has a repercussion which is that we predict a  $J^P = 1/2^-$  state with mass 2615 MeV and zero width, in addition to the state associated to the experimental one at 2592 MeV. We, thus, get two narrow states, one at 2592 MeV and the other one at 2615 MeV. In this range only one narrow state is obtained in Ref. [8] at 2618 MeV.

In order to understand the meaning of the results that we obtain we show in Tables XI to XV the residues,  $g_i$ , and wave function at the origin,  $g_i G_i$  [45]. In Table XI, corresponding to the states of Table VIII for  $q_{max} = 638$  MeV, we can see that while both states couple appreciably to  $DN$  and  $\pi\Sigma_c$ , the amount of  $DN$ , measured by its coupling, or better, the wave function at the origin, is bigger for the lower energy state.

2592.0 + i4.5	$DN$	$\pi\Sigma_c$	$\eta\Lambda_c$
$g_i$	9.10 + i4.4	-1.89 - i0.58	0.74 + i0.37
$g_i G_i^{II}$	-25.90 - i12.81	46.93 + i10.26	-5.28 - i2.71
2623.3 + i26.4	$DN$	$\pi\Sigma_c$	$\eta\Lambda_c$
$g_i$	5.69 - i3.76	1.24 + i1.58	0.56 - i0.29
$g_i G_i^{II}$	-18.54 + i10.31	-43.83 - i29.60	-4.44 + i1.94

TABLE XI. The coupling constants to various channels for the poles in the  $I = 0, J = 1/2$  sector of  $DN$  and coupled channels, taking  $q_{max} = 638$  MeV.

It might be surprising to see that the wave function at the origin for  $\pi\Sigma_c$  is rather large, but this is linked to the fact that we are so close to the  $\pi\Sigma_c$  threshold. Indeed, if one recalls the shape of the  $G$  function, we know that  $\text{Re}G$  is negative, with a discontinuity in the derivative at threshold, where it has the minimum (largest  $|\text{Re}G|$ ) (see fig. 4 of Ref. [13]). This also tells that the amount of the wave function of  $\pi\Sigma_c$  at the origin will be very sensitive to small changes in the mass of the state. This is shown in Tables XII, XIII for  $q_{max} = 645, 650$  MeV. A small change of 1-3 MeV in the binding reduces drastically the  $\pi\Sigma_c$  wave function at the origin to the point that the  $DN$  channel wave function becomes largest. The relevance of the channel in physical processes is linked to the value of this wave function but also to external sources, so one can not make a statement *a priori*. The

self-energy provided by each channel is  $g^2G$ , where the  $DN$  channel would dominate, given the much larger value of  $g$ . With the caveat that the  $\pi\Sigma_c$  channel can be relevant in some physical processes, we shall say that this state is dominated by  $DN$ .

2591.2 + $i0$	$DN$	$\pi\Sigma_c$	$\eta\Lambda_c$
$g_i$	5.41 + $i0$	-0.80 + $i0$	0.45 + $i0$
$g_i G_i^{II}$	-15.80 + $i0$	17.52 + $i0$	-3.30 + $i0$
2621.9 + $i28.4$	$DN$	$\pi\Sigma_c$	$\eta\Lambda_c$
$g_i$	5.06 - $i3.18$	1.35 + $i1.44$	0.51 - $i0.24$
$g_i G_i^{II}$	-16.76 + $i8.73$	-45.94 - $i25.86$	-4.08 + $i1.62$

TABLE XII. The coupling constants to various channels for the poles in the  $I = 0, J = 1/2$  sector of  $DN$  and coupled channels, taking  $q_{max} = 645$  MeV.

2588.8 + $i0$	$DN$	$\pi\Sigma_c$	$\eta\Lambda_c$
$g_i$	7.30 + $i0$	-0.94 + $i0$	0.62 + $i0$
$g_i G_i^{II}$	-21.52 + $i0$	19.62 + $i0$	-4.53 + $i0$
2620.9 + $i29.4$	$DN$	$\pi\Sigma_c$	$\eta\Lambda_c$
$g_i$	4.75 - $i2.82$	1.40 + $i1.36$	0.48 - $i0.21$
$g_i G_i^{II}$	-15.90 + $i7.72$	-47.01 - $i23.92$	-3.90 + $i1.41$

TABLE XIII. The coupling constants to various channels for the poles in the  $I = 0, J = 1/2$  sector of  $DN$  and coupled channels, taking  $q_{max} = 650$  MeV.

It is interesting to see that in Table VIII the higher energy state has a width that increases as the energy of the state decreases. This is not intuitive because one has more phase space for decay as the energy increases. Actually this latter case is reflected by the behavior of the lower energy state. The explanation for this anomaly has to be seen in the evolution of the  $\pi\Sigma_c$  component. As we can see in Table XIV, the trend of the width of the states is tied to the size of the  $\pi\Sigma_c$  wave function at the origin, which increases as the energy of the state decreases and we are approaching the  $\pi\Sigma_c$  threshold .

In Table XV we show the couplings and wave functions at the origin for the states found with  $D^*N$  and coupled channels of Table X. The  $J = 1/2$  state at 2615 MeV couples mostly to  $D^*N$ , the  $3/2$  state at 2628 MeV couples mostly to  $D^*N$  and the spin degenerate state at 2959 MeV couples mostly to  $\rho\Sigma_c$ . This is why the box diagram that couples  $D^*N$  with  $DN$  did not have much relevance in this latter case.

It is instructive to compare the results obtained here with those of Ref. [8]. There a  $1/2^-$ ,  $I=0$  state is found at 2618 MeV, with very small width, which is associated to the  $\Lambda_c(2595)$ . The state couples both to  $DN$  and  $D^*N$  but the coupling to  $D^*N$  is about 50 % bigger than the one to  $DN$ . As we have discussed here, this does not mean that the  $D^*N$  channel is the dominant in the wave function, because what matters is the wave function at the origin,  $gG$ , and, since the  $D^*N$  channel is farther away in energy than the  $DN$ , the  $G$  function is smaller and finally the  $DN$  channel stands as dominant, which would be in agreement with our statement in this paper. It is also interesting to note that in Ref. [8] another  $\Lambda_c$

$2685.5 + i5.2$ ( $q_{max} = 600$ )	$DN$	$\pi\Sigma_c$	$\eta\Lambda_c$
$g_i$	$7.53 - i0.45$	$0.09 + i0.64$	$0.83 - i0.03$
$g_i G_i^{II}$	$-25.83 + i1.01$	$-10.10 - i11.44$	$-6.78 + i0.11$
$2661.8 + i8.7$ ( $q_{max} = 638$ )	$DN$	$\pi\Sigma_c$	$\eta\Lambda_c$
$g_i$	$7.85 - i0.89$	$0.21 + i0.90$	$0.87 - i0.06$
$g_i G_i^{II}$	$-27.73 + i2.32$	$-14.60 - i17.31$	$-7.36 + i0.36$
$2629.4 + i21.5$ ( $q_{max} = 700$ )	$DN$	$\pi\Sigma_c$	$\eta\Lambda_c$
$g_i$	$6.04 - i2.26$	$1.08 + i1.24$	$0.71 - i0.20$
$g_i G_i^{II}$	$-23.35 + i7.17$	$-38.74 - i23.17$	$-6.57 + i1.49$
$2616.7 + i25.7$ ( $q_{max} = 750$ )	$DN$	$\pi\Sigma_c$	$\eta\Lambda_c$
$g_i$	$4.17 - i1.02$	$1.50 + i0.97$	$0.52 - i0.08$
$g_i G_i^{II}$	$-17.57 + i3.09$	$-49.78 - i16.77$	$-5.28 + i0.47$

TABLE XIV. The couplings corresponding to the higher energy state of Table VIII as a function of  $q_{max}$ . (Units: MeV)

$2615.4 + i0$	$D^*N$	$\rho\Sigma_c$	$\omega\Lambda_c$	$\phi\Lambda_c$
$g_i$	10.35	-0.63	0.55	-0.77
$g_i G_i^{II}$	-33.61	3.45	-3.59	3.31
$2959.1 + i0.7$	$D^*N$	$\rho\Sigma_c$	$\omega\Lambda_c$	$\phi\Lambda_c$
$g_i$	$0.22 + i0.12$	$5.36 + i0.01$	$0.07 + i0.02$	$-0.10 - i0.02$
$g_i G_i^{II}$	$-2.96 - i0.71$	$-47.00 - i0.16$	$-0.91 - i0.22$	$0.65 + i0.16$
$2628.5 + i0$	$D^*N$	$\rho\Sigma_c$	$\omega\Lambda_c$	$\phi\Lambda_c$
$g_i$	9.77	-0.64	0.54	-0.76
$g_i G_i^{II}$	-32.44	3.52	-3.59	3.29
$2958.6 + i1.5$	$D^*N$	$\rho\Sigma_c$	$\omega\Lambda_c$	$\phi\Lambda_c$
$g_i$	$0.16 + i0.16$	$5.37 + i0.01$	$0.06 + i0.03$	$-0.08 - i0.05$
$g_i G_i^{II}$	$-2.43 - i1.42$	$-46.99 - i0.20$	$-0.74 - i0.44$	$0.53 + i0.31$

TABLE XV. The coupling constants to various channels for the poles in the  $I = 0, J = 1/2, 3/2$  sector of  $D^*N$  and coupled channels, taking  $q_{max} = 791$  MeV.

resonance is found around 2617 MeV, but with a width of 90 MeV. We also find a similar state around 2623 MeV and a width of 52 MeV. In both cases, a considerable coupling to the  $\pi\Sigma_c$  state is responsible for the width. In addition, in Ref. [8] a state with  $J^P = 3/2^-$ ,  $I = 0$  is obtained at 2666 MeV with a width of 54 MeV which is associated to the  $\Lambda_c(2625)$ . We, instead, get a state at 2628 MeV and with zero width, with the dominant coupling to the  $D^*N$  state, while in Ref. [8] there is a large coupling to  $D^*N$  but there is also some coupling to  $\pi\Sigma_c^*$  which is responsible for the relatively large width. Yet, the width can be drastically reduced if the mass goes down, getting closer to the threshold mass of the  $\pi\Sigma_c^*$  channel (2664 MeV). The dynamics of our approach highly suppresses this latter channel,

which would involve  $D$  exchange instead of  $\pi$  exchange, and is hence further suppressed than the already suppressed pion exchange. Also in the  $J^P = 1/2^-, I = 0$  sector, in Ref. [8] a state with 2828 MeV and a width of 0.8 MeV is found, which couples to  $\rho\Sigma_c$  among other channels. We find a similar state at 2958 MeV of dominant  $\rho\Sigma_c$  nature, with a width of about 2 MeV.

The result obtained here for the  $\Lambda_c(2595)$  also agrees qualitatively with the one in Ref. [21] or Ref. [19], where also the Weinberg Tomozawa interaction is used, with some small differences in the coupling constants and the use of extra channels in Ref. [21] which are farther away in energy and which we have ignored. The important thing is that in these works, the state associated to the  $\Lambda_c(2595)$  couples mostly to  $DN$ , like in our case.

In addition, the results for the single channel  $\pi\Sigma_c^*$  in  $I = 0$  and  $J = 3/2$  are shown in Table XVI.

$q_{max}$	638	700	800	1000	1200
no box	2667.88 + $i$ 36.2	2664.05 + $i$ 28.5	2657.26 + $i$ 17.1	2655.61 + $i$ 0	2646.76 + $i$ 0

TABLE XVI. Poles in single channel  $\pi\Sigma_c^*(2656)$  with  $I = 0$  and  $J = 3/2$  as a function of  $q_{max}$ . (The number in bracket after the channel indicate the mass of the channel. Units: MeV)

We can see that depending on the value of the cut off we get a state barely above threshold or below. In the first case we have a width and in the second the width is zero. By looking at table III of Ref. [8] this state is likely to be identified to the  $3/2$  state at 2666 MeV of Ref. [8] which couples strongly to  $\pi\Sigma_c^*$  and was associated there to the experimental state at 2628 MeV. In our case the state associated to the experimental  $3/2$  has a different nature and is mostly a  $D^*N$  state. If we force the state in Table XVI to correspond to the experimental one with  $J = 3/2$  we need  $q_{max} = 1530$  MeV, which we could not justify with the ranges found from phenomenology. We stick to the choice of the cut off  $q_{max} = 638$  MeV for the  $PB$  channels in which case we have a prediction of a state with  $I = 0$ ,  $J = 3/2$  of 2668 MeV with  $\Gamma = 72$  MeV. We should note that we have obtained a resonant state above threshold with a single channel. This might seem to contradict the findings in Ref. [47] where a single channel with an energy independent potential does not generate resonances above threshold. We have checked that it is the energy dependence of the potential of Eq. (1) what makes the appearance of the state possible. Indeed, if we make the potential energy independent by taking its value at the  $\pi\Sigma_c^*$  threshold we do not get poles above threshold.

### VIII. $I = 1$ STATES

In this section we show the results that we obtain for  $I = 1$  from the  $DN$ ,  $D^*N$ ,  $D\Delta$  and  $D^*\Delta$  and coupled channels.

In Table XVII we show the pole positions of the states obtained with the  $DN$  and coupled channels as a function of the cut off. The idea is that we shall now use the same cut off as for  $I = 0$  with the  $DN$  channel. Depending on the cut off we find one or two poles. When we take  $q_{max} = 638$  MeV, there is only one pole. The 2nd pole gets closer to the  $DN$  threshold and disappears.



$q_{max}$	600	630	638	700	750
no box	$2668.9 + i119.0$	$2669.1 + i113.6$	$2669.1 + i112.1$	$2668.1 + i100.7$	$2666.2 + i91.4$
	–	–	–	$2801.9 + i11.5$	$2795.4 + i16.4$

TABLE XVII. Poles in the  $I = 1$  sector of  $DN$  and coupled channels as a function of  $q_{max}$ . Threshold masses:  $DN(2806)$ ,  $\pi\Sigma_c(2592)$ ,  $\pi\Lambda_c(2425)$ ,  $\eta\Sigma_c(3001)$ . (Units: MeV)

By taking the pole obtained for  $q_{max} = 638$  MeV we show in Table XVIII the couplings and wave functions at the origin. We observe that the state largely couples to  $\pi\Sigma_c$ .

$2669.1 + i112.1$	$DN$	$\pi\Sigma_c$	$\pi\Lambda_c$	$\eta\Sigma_c$
$g_i$	$-1.33 - i0.79$	$1.72 + i1.44$	$0.05 + i0.08$	$0.04 + i0.07$
$g_i G_i^{II}$	$3.18 + i4.01$	$-75.77 - i15.68$	$-3.36 - i0.32$	$-0.17 - i0.48$

TABLE XVIII. The coupling constants to various channels for the poles in the  $I = 1$  sector of  $DN$  and coupled channels, taking  $q_{max} = 638$  MeV.

In Table XIX we show the states obtained with  $D^*N$  and its coupled channels as a function of the cut off. We find two states with zero or a small width. The couplings of these states to the coupled channels are shown in Table XX for the cut off that we used with the same  $D^*N$  channel in  $I = 0$ . We see that the state found around 2917 MeV couples mostly to  $D^*N$ , while the one at 3125 MeV couples mostly to  $\rho\Sigma_c$ .

$q_{max}$	750	780	791	810	850
no box	$2926.4 + i0$	$2920.1 + i0$	$2917.6 + i0$	$2913.0 + i0$	$2902.4 + i0$
	$3141.0 + i3.8$	$3129.9 + i4.2$	$3125.8 + i4.4$	$3118.6 + i4.6$	$3103.1 + i5.0$

TABLE XIX. Poles in the  $I = 1$  sector of  $D^*N$  and coupled channels as a function of  $q_{max}$ . Threshold masses:  $D^*N(2948)$ ,  $\rho\Sigma_c(3229)$ ,  $\rho\Lambda_c(3062)$ ,  $\omega\Sigma_c(3236)$ ,  $\phi\Sigma_c(3173)$ . (Units: MeV)

$2917.62 + i0$	$D^*N$	$\rho\Sigma_c$	$\rho\Lambda_c$	$\omega\Sigma_c$	$\phi\Sigma_c$
$g_i$	3.90	-0.95	-0.71	-0.38	0.53
$g_i G_i^{II}$	-30.90	7.68	8.22	3.04	-2.64
$3125.8 + i4.4$	$D^*N$	$\rho\Sigma_c$	$\rho\Lambda_c$	$\omega\Sigma_c$	$\phi\Sigma_c$
$g_i$	$-0.05 + i0.55$	$3.82 - i0.08$	$-0.17 - i0.11$	$-0.09 - i0.06$	$0.13 + i0.08$
$g_i G_i^{II}$	$-6.26 - i3.91$	$-51.06 + i0.32$	$5.95 - i0.19$	$1.21 + i0.79$	$-0.87 - i0.56$

TABLE XX. The coupling constants to various channels for the poles in the  $I = 1$  sector of  $D^*N$  and coupled channels, taking  $q_{max} = 791$  MeV.

In Table XXI we show the states that we obtain in the  $D\Delta$  and coupled channels. We obtain two states. Once again we use the cut off corresponding to the pseudoscalar-baryon

channels and show the coupling of these states to the different channels in Table XXII. We see that the state that we get at 2736 MeV couples mostly to  $\pi\Sigma_c^*$ , while the one at 2789 MeV couples mostly to  $D\Delta$ .

$q_{max}$	600	630	638	700	750
no box	$2733.9 + i119.4$	$2734.5 + i113.7$	$2734.7 + i112.1$	$2737.6 + i99.2$	$2743.1 + i93.0$
	$2882.0 + i3.1$	$2851.9 + i4.2$	$2843.5 + i4.5$	$2774.4 + i8.1$	$2712.8 + i6.7$
with box	$2734.4 + i119.2$	$2735.6 + i113.4$	$2736.0 + i111.9$	$2740.6 + i102.4$	$2741.2 + i98.2$
	$2829.7 + i3.3$	$2798.0 + i4.5$	$2789.1 + i4.8$	$2714.2 + i4.7$	$2653.9 + i0.2$

TABLE XXI. Poles in the  $I = 1$  sector of  $D\Delta$  and coupled channels as a function of  $q_{max}$ . Threshold masses:  $D\Delta(3099)$ ,  $\pi\Sigma_c^*(2656)$ ,  $\eta\Sigma_c^*(3066)$ . (Units: MeV)

$2736.0 + i111.9$	$D\Delta$	$\pi\Sigma_c^*$	$\eta\Sigma_c^*$
$g_i$	$0.93 + i2.37$	$1.73 + i1.48$	$0.01 + i0.16$
$g_i G_i^{II}$	$-0.96 - i5.50$	$-76.89 - i16.36$	$0.16 - i0.95$
$2789.1 + i4.8$	$D\Delta$	$\pi\Sigma_c^*$	$\eta\Sigma_c^*$
$g_i$	$10.64 - i0.18$	$0.33 - i0.43$	$0.82 - i0.01$
$g_i G_i^{II}$	$-26.55 + i0.19$	$0.54 + i13.73$	$-5.49 - i0.05$

TABLE XXII. The coupling constants to various channels for the poles in the  $I = 1$  sector of  $D\Delta$  and coupled channels, with box and taking  $q_{max} = 638$  MeV.

Finally, in Table XXIII we show the states that we get from the  $D^*\Delta$  and coupled channels. We get two states with zero or a small width. Once again, taking the cut off corresponding to the vector-baryon channels, we show in Table XXIV the coupling to the different channels. We find that the state at 2749 MeV couples mostly to  $D^*\Delta$ , while the one at 3185 MeV couples most strongly to  $\rho\Sigma_c^*$ .

$q_{max}$	750	780	791	810	850
no box	$2852.1 + i0$	$2816.9 + i0$	$2803.9 + i0$	$2781.5 + i0$	$2734.5 + i0$
	$3201.4 + i0$	$3189.7 + i0$	$3185.4 + i0$	$3177.7 + i0$	$3161.3 + i0$
with box	$2791.1 + i0$	$2761.0 + i0$	$2749.2 + i0$	$2728.4 + i0$	$2683.2 + i0$
	$3201.2 + i1.3$	$3189.3 + i1.2$	$3184.9 + i1.1$	$3177.1 + i1.1$	$3160.6 + i1.0$

TABLE XXIII. Poles in the  $I = 1$  sector of  $D^*\Delta$  and coupled channels as a function of  $q_{max}$ . Threshold masses:  $D^*\Delta(3241)$ ,  $\rho\Sigma_c^*(3293)$ ,  $\omega\Sigma_c^*(3301)$ ,  $\phi\Sigma_c^*(3538)$ . (Units: MeV)

We have obtained seven states with  $I = 1$ , corresponding to  $\Sigma_c$  states. In Ref. [8] one also sees three  $\Sigma_c$  states with  $J = 1/2$  and two states with  $J = 3/2$ . Some of them have

$2749.2 + i0$	$D^*\Delta$	$\rho\Sigma_c^*$	$\omega\Sigma_c^*$	$\phi\Sigma_c^*$
$g_i$	11.20	0.44	0.52	0.73
$g_i G_i^{II}$	-31.69	-2.58	-3.04	-2.88
$3184.9 + i1.1$	$D^*\Delta$	$\rho\Sigma_c^*$	$\omega\Sigma_c^*$	$\phi\Sigma_c^*$
$g_i$	$-0.29 - i0.15$	$3.91 - i0.01$	$-0.06 - i0.03$	$0.09 + i0.04$
$g_i G_i^{II}$	$2.32 + i1.17$	$-51.49 - i0.05$	$0.79 + i0.40$	$-0.57 - i0.29$

TABLE XXIV. The coupling constants to various channels for the poles in the  $I = 1$  sector of  $D^*\Delta$  and coupled channels, with box and taking  $q_{max} = 791$  MeV.

strong couplings to particular channels, as we also find here, but the masses of the states differ somewhat. The stronger resemblance is for a state that couples strongly to  $\pi\Sigma_c^*$  in Ref. [8] at 2693 MeV with  $\Gamma = 67$  MeV, while here we find it at 2736 MeV with  $\Gamma = 224$  MeV.

It is curious to see that the  $D^*\Delta$  state has smaller mass than the corresponding  $D^*N$  state, in spite of the  $\Delta - N$  mass difference. The reason has to be seen in the factor 4 in Table VII for  $D^*\Delta \rightarrow D^*\Delta$  versus the factor 1 for  $D^*N \rightarrow D^*N$  in Table VI.

## IX. SUMMARY OF THE RESULTS

Finally, since we have many intermediate results, we summarize here the final results that we get for the states. The results are shown in Table XXV, where we also write for reference the main channel of the state.

main channel	$J$	$I$	$(E, \Gamma)$ [MeV]	Exp.
$DN, \pi\Sigma_c$	1/2	0	2592, 9	$\Lambda_c(2595)$
$\pi\Sigma_c$	1/2	0	2623, 53	-
$D^*N$	1/2	0	2615, 0	-
$D^*N$	3/2	0	2628, 0	$\Lambda_c(2625)$
$\pi\Sigma_c^*$	3/2	0	2668, 70	-
$\rho\Sigma_c$	1/2, 3/2	0	2959, 3	$\Lambda_c(2940)?$
$\pi\Sigma_c$	1/2	1	2669, 224	-
$D\Delta$	3/2	1	2789, 9	-
$\pi\Sigma_c^*$	3/2	1	2736, 224	-
$D^*N$	1/2, 3/2	1	2917, 0	-
$\rho\Sigma_c$	1/2, 3/2	1	3126, 9	-
$D^*\Delta$	1/2, 3/2, 5/2	1	2749, 0	-
$\rho\Sigma_c^*$	1/2, 3/2, 5/2	1	3185, 2	-

TABLE XXV. Energies and widths of the states obtained and the channels to which the states couple most strongly.

In summary, we predict six states with  $I = 0$ , two of them corresponding to the  $\Lambda_c(2595)$  and  $\Lambda_c(2625)$ , and seven states with  $I = 1$ , some of them degenerate in spin. The energies of the states range from about 2592 MeV to 3185 MeV.

It might seem at first sight that this is a large number of states, but we must recall that for the analogous sector of baryon strange states one finds within the same range of difference of energies six  $\Lambda$  states with spin and parity  $J^P = 1/2^-, 3/2^-, 5/2^-$  and six  $\Sigma$  states with the same spin and parity, most of which could be reproduced as dynamically generated states of meson-baryon or vector-baryon [35, 46].

For the moment there is only one  $\Sigma_c$  state reported in the Ref. [28] around 2800 MeV. The state, however, has no spin nor parity assigned. While there are several states in Table XXV close in energy to this state, it is worth quoting that the width of the experimental state is around 75 MeV, which is far away from the  $\Gamma = 0, 9, 224$  MeV, that we find for the likely states in Table XXV according to the mass. We would tentatively conclude that the experimental state corresponds most likely to a positive parity state. On the other hand, the reported state  $\Lambda_c(2940)$  with  $\Gamma = 17_{-6}^{+8}$  MeV [28] which has no spin parity associated, could correspond to the spin degenerate  $\Lambda_c$  state that we find at 2959 MeV with small width. In other approaches that use a constituent quark model [48] a  $D^*N$  structure is suggested for this state. However, as shown in Table XV, this state, which has some coupling to  $D^*N$ , couples mostly to  $\rho\Sigma_c$ . The states dominated by  $D^*N$  in our approach appear more bound.

## X. CONCLUSIONS

In this work we studied the interaction of  $DN$ ,  $D\Delta$ ,  $D^*N$  and  $D^*\Delta$  states with its coupled channels using dynamics extrapolated from the light quark sector to the heavy one. The starting point was to consider the heavy quarks as spectators in the dominant terms of the interaction. The source of interaction was pion exchange, that mixes states of pseudoscalar-baryon with those of vector baryon, and vector exchange. The interaction was extracted mapping from the light sector and respecting the rules of heavy quark spin symmetry. Hence, an extrapolation of the results of the local hidden gauge approach was used. With these elements of the interaction, adding subleading terms in the large heavy quark mass counting, obtained from the exchange of heavy vectors in the local hidden gauge approach, we studied the interaction of the  $DN$ ,  $D\Delta$ ,  $D^*N$  and  $D^*\Delta$  with their coupled channels  $\pi\Sigma_c$ ,  $\pi\Lambda_c$ ,  $\eta\Sigma_c$  (for the  $DN$ );  $\pi\Sigma_c^*$ ,  $\eta\Sigma_c^*$  (for the  $D\Delta$ );  $\rho\Sigma_c$ ,  $\omega\Lambda_c$ ,  $\phi\Lambda_c$ ,  $\rho\Sigma_c^*$ ,  $\omega\Sigma_c^*$ ,  $\phi\Sigma_c^*$  (for the  $D^*N$ ); and  $\rho\Sigma_c^*$ ,  $\omega\Sigma_c^*$ ,  $\phi\Sigma_c^*$  (for the  $D^*\Delta$ ), and we searched for poles of the scattering matrix in different states of spin and isospin. We found six states in  $I = 0$ , with one of them degenerate in spin  $J = 1/2$ ,  $3/2$ , and seven states in  $I = 1$ , two of them degenerate in spin  $J = 1/2$ ,  $3/2$ , and two more degenerate in spin  $J = 1/2$ ,  $3/2$ ,  $5/2$ . The coupling of the states to the different channels, together with their wave function at the origin, were evaluated to show which is the weight of the different building blocks in those molecular states. In particular, two of the states, one with spin  $1/2$  that couples mostly to  $DN$ , and a second one with spin  $3/2$  that couples mostly to  $D^*N$  were associated to the experimental ones,  $\Lambda_c(2595)$  and  $\Lambda_c(2625)$  respectively. The rest of states are so far predictions, with a number of states that is similar to the one of negative parity  $\Lambda$  and  $\Sigma$  states in the strange sector. We think that the use of realistic dynamics, with strict respect of heavy quark spin-flavor symmetry, renders the results obtained rather solid and they should serve as a guideline for future experiments searching for baryon states with open charm.

## ACKNOWLEDGMENTS

This work is partly supported by the Spanish Ministerio de Economía y Competitividad and European FEDER funds under Contract No. FIS2011-28853-C02-01 and the Generalitat Valenciana in the program Prometeo, 2009/090. We acknowledge the support of the European Community-Research Infrastructure Integrating Activity Study of Strongly Interacting Matter (Hadron Physics 3, Grant No. 283286) under the Seventh Framework Programme of the European Union. This work is also partly supported by the National Natural Science Foundation of China under Grant No. 11165005.

- 
- [1] N. Isgur and M. B. Wise, Phys. Lett. B **232**, 113 (1989).
  - [2] M. Neubert, Phys. Rept. **245**, 259 (1994) [hep-ph/9306320].
  - [3] A.V. Manohar and M.B. Wise. Heavy Quark Physics, Cambridge Monographs on Particle Physics, Nuclear Physics and Cosmology, vol. 10. Camb. Monogr. Part. Phys. Nucl. Phys. Cosmol.10,1
  - [4] M. B. Wise, Phys. Rev. D **45**, 2188 (1992).

- [5] C. Garcia-Recio, V. K. Magas, T. Mizutani, J. Nieves, A. Ramos, L. L. Salcedo and L. Tolos, Phys. Rev. D **79**, 054004 (2009) [arXiv:0807.2969 [hep-ph]].
- [6] J. M. Flynn, E. Hernandez and J. Nieves, Phys. Rev. D **85**, 014012 (2012) [arXiv:1110.2962 [hep-ph]].
- [7] C. Garcia-Recio, J. Nieves, O. Romanets, L. L. Salcedo and L. Tolos, Phys. Rev. D **87**, 034032 (2013) [arXiv:1210.4755 [hep-ph]].
- [8] O. Romanets, L. Tolos, C. Garcia-Recio, J. Nieves, L. L. Salcedo and R. G. E. Timmermans, Phys. Rev. D **85**, 114032 (2012) [arXiv:1202.2239 [hep-ph]].
- [9] F. -K. Guo, C. Hidalgo-Duque, J. Nieves and M. P. Valderrama, Phys. Rev. D **88**, 054014 (2013) [arXiv:1305.4052 [hep-ph]].
- [10] C. W. Xiao, J. Nieves and E. Oset, Phys. Rev. D **88**, 056012 (2013) [arXiv:1304.5368 [hep-ph]].
- [11] C. Garcia-Recio, J. Nieves, O. Romanets, L. L. Salcedo and L. Tolos, Phys. Rev. D **87**, 074034 (2013) [arXiv:1302.6938 [hep-ph]].
- [12] O. Romanets, L. Tolos, C. Garcia-Recio, J. Nieves, L. L. Salcedo and R. Timmermans, Nucl. Phys. A **914**, 488 (2013) [arXiv:1212.3943 [hep-ph]].
- [13] C. W. Xiao and E. Oset, Eur. Phys. J. A **49**, 139 (2013) [arXiv:1305.0786 [hep-ph]].
- [14] M. Bando, T. Kugo, S. Uehara, K. Yamawaki and T. Yanagida, Phys. Rev. Lett. **54**, 1215 (1985).
- [15] M. Bando, T. Kugo and K. Yamawaki, Phys. Rept. **164**, 217 (1988).
- [16] U. G. Meissner, Phys. Rept. **161**, 213 (1988).
- [17] H. Nagahiro, L. Roca, A. Hosaka and E. Oset, Phys. Rev. D **79**, 014015 (2009) [arXiv:0809.0943 [hep-ph]].
- [18] W. H. Liang, C. W. Xiao and E. Oset, arXiv:1401.1441 [hep-ph].
- [19] M. F. M. Lutz and C. L. Korpa, Phys. Lett. B **633**, 43 (2006) [nucl-th/0510006].
- [20] L. Tolos, J. Schaffner-Bielich and H. Stoecker, Phys. Lett. B **635**, 85 (2006) [nucl-th/0509054].
- [21] T. Mizutani and A. Ramos, Phys. Rev. C **74**, 065201 (2006) [hep-ph/0607257].
- [22] L. Tolos, A. Ramos and T. Mizutani, Phys. Rev. C **77**, 015207 (2008) [arXiv:0710.2684 [nucl-th]].
- [23] J. -J. Wu, R. Molina, E. Oset and B. S. Zou, Phys. Rev. Lett. **105**, 232001 (2010) [arXiv:1007.0573 [nucl-th]].
- [24] J. -J. Wu, R. Molina, E. Oset and B. S. Zou, Phys. Rev. C **84**, 015202 (2011) [arXiv:1011.2399 [nucl-th]].
- [25] J. -J. Wu and B. S. Zou, Phys. Lett. B **709**, 70 (2012) [arXiv:1011.5743 [hep-ph]].
- [26] J. Haidenbauer, G. Krein, U. -G. Meissner and A. Sibirtsev, Eur. Phys. J. A **33**, 107 (2007) [arXiv:0704.3668 [nucl-th]].
- [27] J. Haidenbauer, G. Krein, U. -G. Meissner and L. Tolos, Eur. Phys. J. A **47**, 18 (2011) [arXiv:1008.3794 [nucl-th]].
- [28] J. Beringer *et al.* [Particle Data Group Collaboration], Phys. Rev. D **86**, 010001 (2012).
- [29] E. Oset and A. Ramos, Nucl. Phys. A **635**, 99 (1998) [nucl-th/9711022].
- [30] S. Sarkar, E. Oset and M. J. Vicente Vacas, Nucl. Phys. A **750**, 294 (2005) [Erratum-ibid. A **780**, 78 (2006)] [nucl-th/0407025].
- [31] E. Oset, A. Ramos and C. Bennhold, Phys. Lett. B **527**, 99 (2002) [Erratum-ibid. B **530**, 260 (2002)] [nucl-th/0109006].
- [32] E. Oset and A. Ramos, Eur. Phys. J. A **44**, 445 (2010) [arXiv:0905.0973 [hep-ph]].
- [33] S. Sarkar, B. -X. Sun, E. Oset and M. J. Vicente Vacas, Eur. Phys. J. A **44**, 431 (2010) [arXiv:0902.3150 [hep-ph]].

- [34] E. J. Garzon and E. Oset, *Eur. Phys. J. A* **48**, 5 (2012) [arXiv:1201.3756 [hep-ph]].
- [35] E. Oset, A. Ramos, E. J. Garzon, R. Molina, L. Tolos, C. W. Xiao, J. J. Wu and B. S. Zou, *Int. J. Mod. Phys. E* **21**, 1230011 (2012) [arXiv:1210.3738 [nucl-th]].
- [36] K. P. Khemchandani, A. Martinez Torres, H. Kaneko, H. Nagahiro and A. Hosaka, *Phys. Rev. D* **84**, 094018 (2011) [arXiv:1107.0574 [nucl-th]].
- [37] K. P. Khemchandani, H. Kaneko, H. Nagahiro and A. Hosaka, *Phys. Rev. D* **83**, 114041 (2011) [arXiv:1104.0307 [hep-ph]].
- [38] A. Ozpineci, C. W. Xiao and E. Oset, *Phys. Rev. D* **88**, 034018 (2013) [arXiv:1306.3154 [hep-ph]].
- [39] B. Borasoy, *Phys. Rev. D* **59**, 054021 (1999) [hep-ph/9811411].
- [40] R. C. Carrasco and E. Oset, *Nucl. Phys. A* **536**, 445 (1992).
- [41] E. Oset and M. J. Vicente-Vacas, *Nucl. Phys. A* **446**, 584 (1985).
- [42] E. Oset, H. Toki and W. Weise, *Phys. Rept.* **83**, 281 (1982).
- [43] D. Jido, J. A. Oller, E. Oset, A. Ramos and U. G. Meissner, *Nucl. Phys. A* **725**, 181 (2003) [nucl-th/0303062].
- [44] P. Gonzalez, E. Oset and J. Vijande, *Phys. Rev. C* **79**, 025209 (2009) [arXiv:0812.3368 [hep-ph]].
- [45] D. Gamermann, J. Nieves, E. Oset and E. Ruiz Arriola, *Phys. Rev. D* **81**, 014029 (2010) [arXiv:0911.4407 [hep-ph]].
- [46] J. A. Oller, E. Oset and A. Ramos, *Prog. Part. Nucl. Phys.* **45**, 157 (2000) [hep-ph/0002193].
- [47] J. Yamagata-Sekihara, J. Nieves and E. Oset, *Phys. Rev. D* **83**, 014003 (2011) [arXiv:1007.3923 [hep-ph]].
- [48] P. G. Ortega, D. R. Entem and F. Fernandez, *Phys. Lett. B* **718**, 1381 (2013) [arXiv:1210.2633 [hep-ph]].